buildings

MDPI

Article

Outdoor Characterization of Phase Change Materials and Assessment of Their Energy Saving Potential to Reach NZEB

Cristina Cornaro [1,*], Marco Pierro [1,2], Valerio Adoo Puggioni [3] and Daniele Roncarati [1]

1 Department of Enterprise Engineering, University of Rome 'Tor Vergata', Via del Politecnico, 1, 00133 Rome, Italy; marco.pierro@uniroma2.it (M.P.); daniele.roncarati3@gmail.com (D.R.)
2 Institute for Renewable Energy, EURAC Research, Bolzano 39100, Italy
3 EnUp srl, Via dei Monti di Primavalle, 151, 00168 Rome, Italy; puggioni@enup.it
* Correspondence: cornaro@uniroma2.it; Tel.: +39-06-7259-7233

Received: 7 April 2017; Accepted: 17 June 2017; Published: 22 June 2017

Abstract: Phase change materials (PCM) are very promising materials for improving energy efficiency in buildings, especially in hot weather conditions. In spite of the growing attention paid to the integration of PCM into buildings, there are few studies on PCM evaluation under real operating conditions. This lack of data often does not allow accurate calibration and validation of building simulation models. This work aims to characterize a commercial PCM panel by RUBITHERM®. The panel was laid on the floor of a test box exposed outdoors, and the experimental data were used to validate a PCM software tool implemented in IDA Indoor Climate and Energy software. A reference office building model with characteristics prescribed by Italian regulations (STD) was provided with three PCM with melting points of approximately 21 °C, 24 °C and 26 °C, laid on the floor office. The building energy performance obtained was compared to the energy performance of a reference building prescribed by the new Italian building energy performance regulation (NZEB) for three cities in Italy (Trento, Rome and Palermo). The results showed that energy savings obtained from implementing PCM in the STD building were not sufficient to reach the NZEB reference value for all cities. Only the use of night ventilation was able to assist in reaching NZEB. PCM with a 21 °C melting point showed the best annual energy saving performance in all cities. Temperature range and temperature peaks experienced by PCM in the day/night cycle can explain the behavior of these materials in the various cities and seasons as latent and sensible heat storage systems.

Keywords: PCM; dynamic simulation; IDA ICE; outdoor monitoring; validation; NZEB

1. Introduction

Since the 1930s, phase change materials (PCM) have been investigated thanks to the pioneering work of Telkes [1]. Many studies have since been conducted on these materials, but unfortunately, their application did not take off due to technological constraints and costs. However in the last few years, interest for PCM has grown again, and this is confirmed by the recent reviews from Khadiran et al. [2], Souayfane et al. [3] and Kenisarin and Mahkamov [4].

Many studies can be found in the literature regarding experimental and theoretical analysis of PCM behavior. It is possible to group these works into laboratory studies, outdoor experimental studies, numerical and theoretical investigations, and studies involving experiments and theory.

Various works could be found concerning laboratory tests. Most of the works examined regard the evaluation of thermal characteristics of gypsum boards containing microencapsulated PCM tested in simulation chambers and/or tests boxes ([5–9]). Barreneche et al. [10] incorporated PCMs with

Portland cement and gypsum and investigated the best PCM quantity for incorporation into each material tested.

For outdoor studies it is worth mentioning Tardieu et al. [11] which used two cabins, built in Auckland, New Zealand, one as a reference and one with PCM, and a numerical simulation using Energy Plus, to evaluate the thermal behavior of the two cabins. Both simulation and experimental data collected showed that PCM in the wallboards improved the thermal inertia of the buildings. From simulations, they also concluded that the additional thermal mass of PCM could reduce daily indoor temperature fluctuation by up to 4 °C in summer days. Also Entrop et al. [12] made experiments using small boxes exposed outdoor in Netherland and equipped with different materials among which also PCM. Their results showed that PCM is an excellent way to store energy and small boxes are effective in studying this aspect. Also Su et al. [13] used a box to evaluate PCM thermal behavior in China while Sage-Lauck and Sailor, [14] built a Passive House duplex in Portland, Oregon. They found that the addition of PCM could reduce the number of hours of over-heating by about 60%.

Goia et al. [15] tested a glazing system filled with PCM in outdoor conditions during a long term monitoring campaign. They concluded that the PCM glazing is capable of smoothening and shifting solar gains, and that this result could positively contribute to the energy balance of highly glazed buildings.

Numerical simulation is also used to evaluate PCM performance at different locations and climates using various simulation tools such as ESP-r [16], self-made programs [17], COMSOL environment [18], and Energy Plus [19]. Ascione et al. [20] confirmed the capability of energy saving by PCM in office buildings during thewarm season in various cities in the Mediterranean area. They varied melting temperature from 26 °C to 29 °C, also varying the PCM layer thickness and configuration. They found little benefit in energy consumption, probably because they tested melting points that were higher than the HVAC temperature set point fixed at 26 °C. Indeed Seong and Lin [21] explored the importance of setting the right melting point to obtain optimal benefits from these kinds of materials, and they evidenced how it is important to stay near the temperature set point to save energy. Moreover they demonstrated how night ventilation is useful to further improve benefits. Even if, as evidenced, various software tools allowed the simulation of PCM behavior in buildings, very few works use experimental data to validate the simulation models [22].

The aim of this work was twofold. The first aim was to characterize the behavior of PCM in real operating conditions through an outdoor experimental test. The data gathered was used to validate the behavior of a custom PCM simulation tool integrated in a whole building simulation software (IDA ICE 4.7.1) [23]. The second aim was to explore the capability of PCM in reducing energy consumption in buildings through dynamic simulation, using the same software validated. For this purpose, an office buildings were located in different Italian cities representative of different climatic zones, and the performance of PCM was evaluated with respect to buildings with NZEB characteristics, used as a reference by the recent Italian norm of minimum requirements [24]. In the following sections, the work method is described, and the outdoor characterization of PCM and the validation of the PCM software tool are presented. The results obtained in terms of energy saving during the year for a reference office building are discussed varying the PCM characteristics at three locations in Italy.

2. Materials and Methods

2.1. Method

The methodology used for this study is schematically shown in Figure 1. The objective was the outdoor characterization of a phase change material commonly used in the building sector, and the evaluation of its capability to reduce heating and cooling loads inside an office building for various climates in Italy.

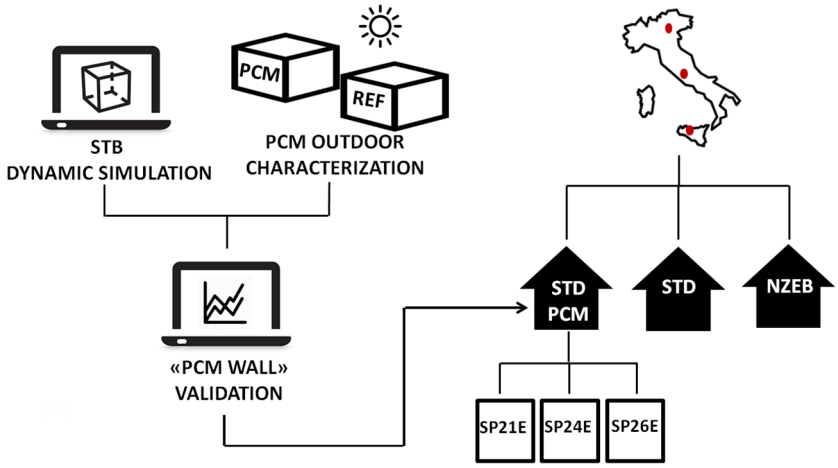

Figure 1. Schematic of methodology used for the study proposed. Red spots show the location of the three cities in which the buildings were tested.

Three locations, Trento, Rome and Palermo, representative of three different climatic zones, were chosen and for each of them, two models of an office building were built in a dynamic simulation environment (IDA ICE 4.7.1 by Equa simulation, Solna, Sweden). The envelope characteristics of one model, named STD building, complied with the prescriptions of the italian norm 192/2005 [25], while the other model envelope complied with the recent minimum requirements norm of 25 June 2015 [24] (NZEB building). STD building was provided with three different kinds of commercial PCM boards with different melting points (SP21E, SP24E, SP26E, specifications provided by RUBITHERM® (Berlin, Germany) and the results on heating and cooling delivered energy were compared to the STD building and the NZEB building to verify possible improvements in energy saving with respect to both references.

For this purpose, a custom software tool named "PCM wall" was implemented in IDA ICE to simulate PCM behavior. The tool validation was carried out before the simulations using experimental data coming from Solar Test Boxes (STBs) used for the outdoor characterization [26]. The devices were built at the ESTER lab of the University of Rome Tor Vergata with the objective of making comparative analysis of thermal and lighting performance of transparent material with respect to a double glass reference pane, and to evaluate the solar heat gain and U-value of innovative semi-transparent materials.

In the present study, they were used to test the thermal performance of a SP21E PCM panel provided by RUBITHERM® with dimensions of 450 mm × 300 mm × 15 mm, and characteristics listed in Table 1. The STBs were provided with two identical standard double glass panes. In the experiments, one of the boxes (PCM) contained the PCM panel, while the other (REF) was used as reference.

Table 1. SP21E phase change material (PCM) panel characteristics.

Data	Value
Melting temperature range	22–23 °C
Solidification temperature range	21–19 °C
Heat storage capacity combination of sensible and latent heat in a temperature range of 13 °C to 28 °C.	160 kJ/kg
Specific heat capacity	2 kJ/kg·K
Density of solid (15 °C)	1.5 kg/L
Density of liquid (35 °C)	1.4 kg/L
Volume expansion	3–4%
Thermal conductivity	0.6 W/mK
Max operation temperature	45 °C

The thermal behavior of STBs was simulated in the IDA ICE dynamic simulation environment. In particular, the "PCM box" model was provided with the custom PCM software module to simulate the PCM panel. Temperature data collected during two short-term outdoor monitoring campaigns, carried out in different periods of the year, were used to validate the results.

2.2. Solar Test Boxes

The boxes (Figure 2a) were designed with a linear scale factor of 1:5 and a surface scale factor of 1:25 with respect to a real room. They have the dimensions of 1.00 m × 0.60 m × 0.55 m and consisted of five opaque walls and one glazed wall. The boxes envelope consisted of plywood panels of 8 mm thickness painted entirely white, to make them highly reflective. Heavy insulation of 80 mm thickness was inserted in the entire non-glazed inner surface of the boxes, also comprising the area behind the frame of the window. On the south facing wall a glazed area of 42 cm × 37 cm can be allocated, the remaining of this surface being occupied by a wood frame 90 mm thick, to shield the thickness of the inside insulating material. Each box was instrumented to measure the inside air temperature, illuminance, and the surface temperature of the inner and outer side of the glazed pane.

(**a**) (**b**)

Figure 2. Solar Test Boxes at ESTER lab: (**a**) Solar test boxes (STBs) in the original configuration with a glazed surface; (**b**) STB used for the present study with a wider frame applied.

TT500 thermistors by Tecno.el srl measure temperature with a wide temperature range (−30 to 120 °C), a resolution of 0.1 °C and an accuracy of ±0.2 °C. Illuminance is measured using a luxmeter by Delta Ohm srl with a measurement range of 200,000 lx, a sensitivity of 1.5 mV/klx, and calibration accuracy of less than 4%. Also, outside temperature and relative humidity, solar irradiance on the vertical plane, and wind speed and direction were measured using a portable weather station.

A Rotronic Hygroclip2 sensor measures temperature and relative humidity with an accuracy of ±0.1 °C for temperature and of ±0.8% for relative humidity. A solar irradiance sensor is a silicon cell pyranometer provided by Apogee Instruments with an accuracy of ±5%, while wind speed and direction are measured using a model 7911 anemometer provided by Davis Instruments with an accuracy of ±1 m/s for speed and of ±7° for direction. Data collection took place at a per-minute time rate.

The weather and solar station of ESTER lab (Latitude 41.9, Longitude 12.6) [27] provides direct and diffuse solar irradiance measurements useful for climate file construction in the dynamic simulation software. Table 2 lists the material properties used in STBs. For the purpose of this study, the glazed surface was reduced to control solar irradiance entering into the boxes. In this way, PCM was not exposed to temperatures high enough to damage it.

For this reason, the original glazed area was reduced using a wider wood frame (Figure 2b). A new calibration was necessary to take this modification into account [28].

Table 2. Thermal properties of STB materials.

Material	Thickness (mm)	Density (kg/m^3)	Specific Heat (J/kg·K)	Thermal Conductivity (W/mK)	Thermal Resistance (m^{2}K/W)	g-Value
Plywood	8	545	1215	0.120	-	-
Insulation	80	36	1453	0.024 (at 10 °C)	3.33	-
Glazing	20	2400	800	1.4	0.34	0.82

2.3. PCM Software Tool

STBs were simulated in the IDA ICE environment. The geographic location corresponded to ESTER lab coordinates, and for all the simulations, customized climate files were built using weather data coming from the weather and solar station of the same lab. Boxes were oriented with the glazed area toward the south. Thermal properties listed in Table 2 were inserted into the model. For the STB provided with the PCM, the custom software module was connected to the STB floor and operated in advanced level mode. Cornaro et al. 2016 [26] gives a more detailed description of all input settings for the STBs simulation.

"PCM wall" is a module for IDA ICE, written in Neutral Model Format language, that allows calculating the heat absorbed and/or released by phase change materials. It uses an enthalpy formulation to describe the relation between enthalpy and temperature for a PCM with different paths during melting and solidification phases. The partial enthalpies and the temperature coordinates are input parameter vectors describing this relation. Partial enthalpies are in J/kg. Heat capacity [J/(kg·K)] is calculated by dividing the partial enthalpy difference at different temperatures by the corresponding temperature interval. The computed help variable "Mode" is used to keep track of current state (phase) of the PCM. Figure 3a shows the enthalpy versus temperature curves, as specified by RUBITHERM® for the SP21E PCM panel (Figure 3b), for melting and solidification. This data was input into the PCM software module.

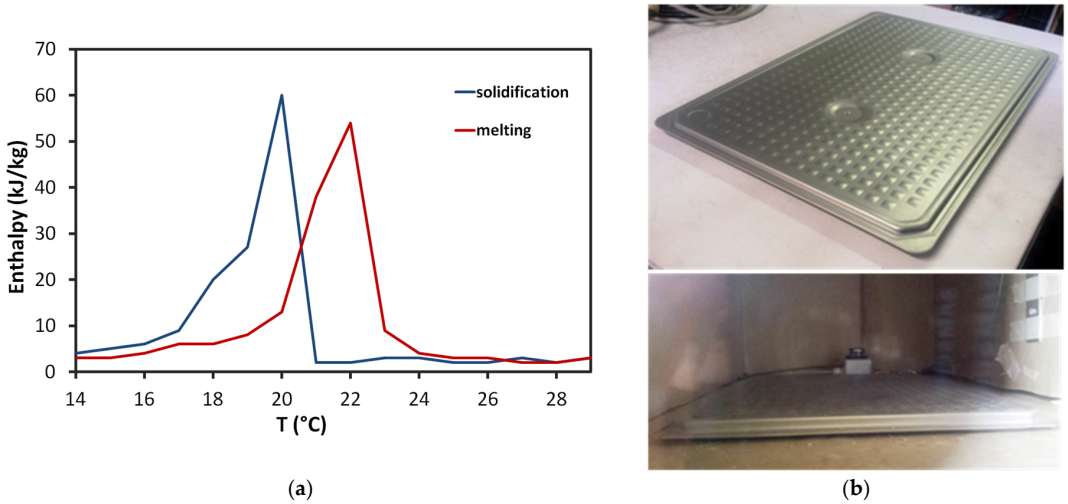

Figure 3. (**a**) Enthalpy—temperature curves for melting and solidification for the SP21E board tested; (**b**) SP21E panel and the panel laid on the STB floor.

2.4. Climate Conditions at the Three Locations

According to the Italian norm [24], Italian cities are grouped into six climate zones depending on their heating and cooling degree-days. These zones are classified from letter "A" to "F", switching from a hot to a cold climate. The three cities selected for this work are representative of three different zones: Trento (F zone), Rome (D zone) and Palermo (B zone). The Koppen and Geiger climate classification [29]

was used to identify the climate of the three cities. Trento city (Latitude 46.07, Longitude 11.13) was classified with the acronym "Cfa", meaning "humid temperate climate" with hot summer (Continental climate), characterized by annual rainfall between 700 mm and 1500 mm. The least amount of rainfall occurs in January. The average in this month is 45 mm. The greatest amount of precipitation occurs in November; with an average of 98 mm. Temperatures are highest in July, with an average of 22.9 °C. The lowest temperatures of the year occur in January, with an average of 1.1 °C.

According to Koppen and Geiger, Rome and Palermo belonged to the "Csa" climate. "Csa" means temperate and hot climate of the middle latitudes with dry and hot summer and cool, rainy winter (Mediterranean climate). The average annual precipitation is around 750 mm.

In Rome (Latitude 41.90, Longitude 12.50), the driest month is July, with 17 mm of rain. Most precipitation falls in November, with an average of 114 mm. July is the warmest month of the year. Average temperature in July is 24.4 °C. In January, the average temperature is 7.7 °C. It is the lowest average temperature of the whole year.

In Palermo (Latitude 38.12, Longitude 13.36), the driest month is July, with 4 mm of rain. Most of the precipitation here falls in December; with 90 mm. August is the warmest month of the year. Average temperature in August is 26.2 °C. January is the coldest month, with temperatures averaging 12.1 °C. Table 3 resumes the main climate features of the three cities.

Table 3. Climate characteristics of the three locations selected for the study.

City	Climate	Annual T_{avg} (°C)	Annual T_{min} (°C)	Annual T_{max} (°C)	Rain (mm)
Trento	Cfa	12.5	7.5	17.6	900
Rome	Csa	15.7	10.7	20.8	798
Palermo	Csa	18.4	15.2	21.7	605

2.5. Reference Buildings

Two reference buildings (STD and NZEB) models where built in the IDA ICE 4.7.1 environment according to the specifications presented in the next sections.

2.5.1. Building Main Features

The reference building used for this study was a well-established model originally defined in the European Commission Joule project REVIS and further refined in the International Energy Agency Solar Heating and Cooling (IEA SHC) program Task 27 (Performance of solar facade components). The European Commission project SWIFT and for International Energy Agency (IEA) Solar Heating and Cooling (SHC) Task 25 (Solar assisted air conditioning of buildings) and Task 31 (Daylighting Buildings in the 21st century) [30] used the same specifications. The authors used it also in a previous work [31]. Figure 4 shows a schematic of one typical floor of the reference building. It comprised 210 office modules, distributed over seven floors and two orientations: 15 office modules per floor, at each of the two orientations (north/south in this study) are separated by a central corridor 3.1 m wide and provided with the staircase/service spaces at both ends of the building. The height of the building was 21 m. The total floor area was 6820 m^2, 974 m^2 for each floor. Each room was a middle-size office, 3.5 m in width and 5.4 m in depth, the height was 2.7 m, and the distance between floors was 3 m. The office was conditioned by a simple fan coil (nominal power 8000 W) coupled to a main plant, one boiler and one chiller (COP 1.67), always on. The fan coil was turned on every working day from 8 a.m. to 7 p.m. To reduce the calculation time, only one office floor was considered for the simulations. Heating and cooling set point temperatures were maximum 20 °C and minimum 12 °C for heating and minimum 26 °C and maximum 28 °C for cooling. These set points were guaranteed during weekdays while during weekends air temperature could not fall below 12 °C in heating and rise above 28 °C for cooling. An infiltration rate of 0.6 Air change per hour (ACH) was also considered for all days of the year.

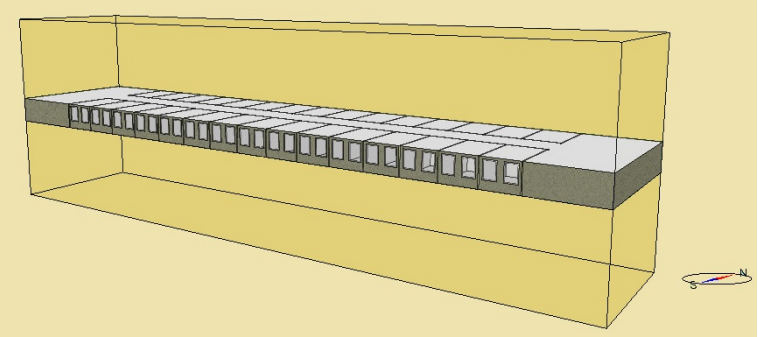

Figure 4. Schematic view of the reference model for an office building.

The space was illuminated by a lighting system with the target work plane illuminance of 500 lx, according to UNI-EN 12464 [32]. The lighting power density in the office was 8 W/m^2 and the space was occupied by two occupants on weekdays from 8 a.m. to 7 p.m.

2.5.2. STD Building

The Standard reference building (STD) represented an Italian building envelope as prescribed by the norm 192/2005 for the year 2006 [25]. The three cities selected for this study: Palermo, Rome and Trento, represented the B, D and F climatic zones, respectively. The thermal and optical properties of the transparent materials and opaque walls shown in Table 4 for the three locations were applied to the building model (Figure 4).

Table 4. Thermal and optical proprieties of the double-glazed element and wall (STD).

City	Materials	U-Value (W/m^2·K)	Tvis	Tsol	g-Value	ε
Trento	Window (Uw)	2.4	0.461	0.382	0.5	0.83
	Wall	0.44	-	-	-	-
Rome	Window (Uw)	3.1	0.461	0.382	0.5	0.83
	Wall	0.50	-	-	-	-
Palermo	Window (Uw)	4.0	0.461	0.382	0.5	0.83
	Wall	0.63	-	-	-	-

2.5.3. NZEB Building

The NZEB building was built referring to the recent Italian norms that fixed the upper limit of thermal transmittance for opaque/transparent surfaces, and the g-value for transparent surfaces according to climate zones by 2019/21 [24]. The thermal and optical properties of the transparent materials and opaque walls shown in Table 5 for the three locations were applied to the building model (Figure 4).

Table 5. Thermal and optical properties of the double glazing element and walls (NZEB).

City	Materials	U-Value (W/m^2·K)	Tvis	Tsol	g-Value	ε
Trento	Window (Uw)	1.1	0.461	0.349	0.35	0.83
	Wall	0.24	-	-	-	-
Rome	Window (Uw)	1.8	0.461	0.349	0.35	0.83
	Wall	0.29	-	-	-	-
Palermo	Window (Uw)	3.0	0.461	0.349	0.35	0.83
	Wall	0.43	-	-	-	-

3. Results

3.1. PCM Oudoor Characterization

Two measurement campaigns were carried out, each including three full days of data acquisition. The first campaign was carried out during the warm season, from the 26th to the 29th of September 2016. Two boxes were exposed outdoors, one with a PCM board layered on the box floor (PCM box, see Figure 3b) and the other one without PCM (REF box). Air temperature inside both boxes was measured together with outdoor air temperature, relative humidity, wind speed and direction, and global irradiance on a vertical plane. Climatic conditions during the test are presented in Figure 5a where air temperature and solar irradiance measured on a vertical plane are showed. Good weather conditions with high temperatures were characteristic of the time period (maximum peak at 29 °C) and there was a significant thermal range between day and night (12–13 °C). Solar irradiance reached peaks of approximately 800 W/m^2. Figure 5b shows the air temperature trends inside the reference box (REF) and the PCM box (PCM) during the test. A significant decrease in maximum temperature was observed in the PCM box with respect to the REF box, due to the PCM melting in the temperature range 22–23 °C. An average decrease of the temperature peaks of approximately 10 °C was observed during the day, while at night an opposite behavior occurred. Indeed, air temperature inside the PCM box was higher than in the REF box due to PCM solidification and thermal mass.

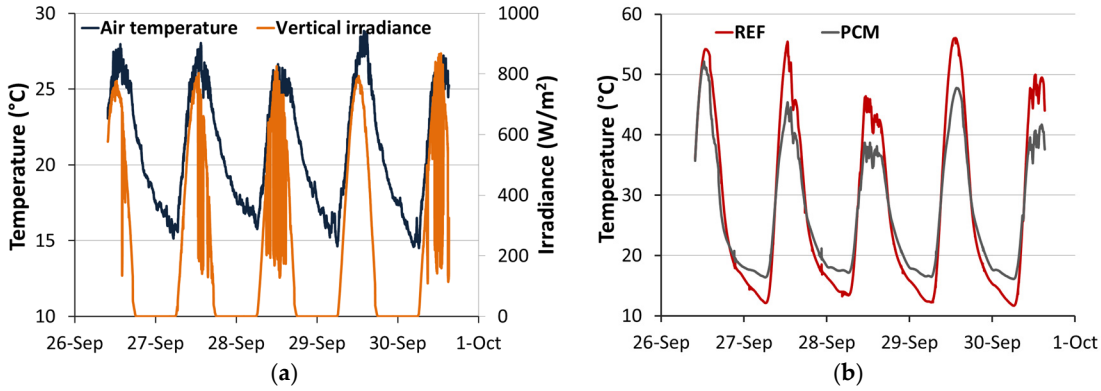

Figure 5. Experimental data from the warm season monitoring campaign: (**a**) trends of outdoor air temperature and global irradiance on a vertical plane; (**b**) trends of air temperature inside the REF box and the PCM box during the test.

No evident shift of the temperature trend due to PCM heat capacity was observed; this was because the amount of material into the box was not enough to produce this effect.

A second measurement campaign was carried on later, between the 5th and the 9th of December 2016 during the cold season. Nice weather was experienced during the last two days of test while the first day was overcast but not rainy, as evidenced by Figure 6a. Outdoor air temperature, in this case, was lower than the first campaign, with a maximum of approximately 21 °C and a minimum of approximately 2 °C with a thermal range of 15 °C in the clear days. Solar irradiance reached values as high as 930 W/m^2. This is because in this period, sun elevation was low, so a vertical surface would receive higher irradiance than a horizontal one. Figure 6b shows the temperature trends inside REF and PCM boxes.

Also in this case, a temperature peak damping of approximately 10 °C caused by the PCM was observed during clear days, while for the overcast day (6th of December), no effect on the material was observed due to the low temperatures experienced inside the box (well below melting point).

PCM solidification occurred earlier in the day (around 7 p.m.) than in the first study (around midnight). Apart from this shift, a change in the curvature of the decreasing temperature trend with

respect to the first study was observed. This was probably due to the behavior of the solid phase at temperatures well below the solidification temperature.

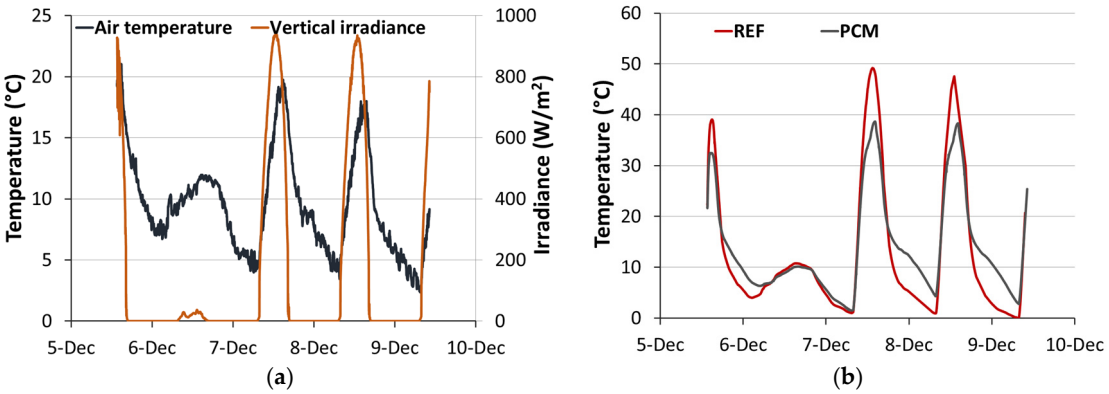

Figure 6. Experimental data from the cold season monitoring campaign: (**a**) trends of outdoor air temperature and global irradiance on a vertical plane; (**b**) trends of air temperature inside the REF box and the PCM box during the test.

Figure 7a,b show the heat fluxes of PCM and of incoming solar radiation, together with the temperature experienced by PCM simulated for the two monitoring campaigns.

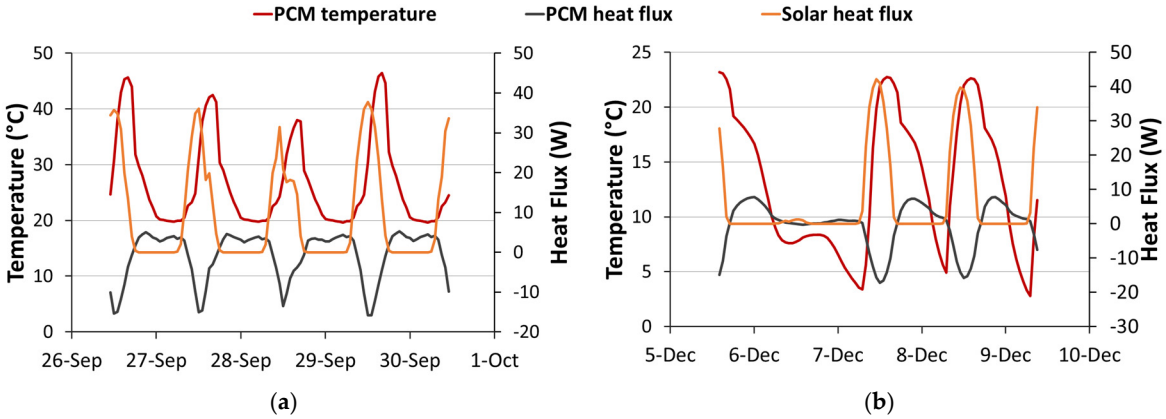

Figure 7. Heat flux of PCM and of incoming solar radiation and temperature trend of the PCM: (**a**) warm season campaign; (**b**) cold season campaign.

The panel removed approximately 15 W peak during the day compared to an incoming solar flux, with peaks of around 40 W (around 40% of heat reduction) lowering the box air temperature peaks by approximately 10 °C.

During the night, it released heat (4–5 W) due to solidification. While during the warm season campaign it stayed in the liquid phase throughout the day, and in solid phase during the night, in the cold season studies, it was mainly in the solid phase due to low outside temperatures, melting occurring only between 11:00 a.m. and 6:00 p.m.

3.2. PCM Software Tool Validation

Validation of the custom PCM software was carried out using experimental data collected during the two experimental campaigns. The two datasets showed different behaviors of the PCM due to the different climatic conditions. During the month of September, the weather was such that the PCM material could work fully in its phase change temperature range, while in the month of December;

even if solar irradiance was high, external air temperature limited the PCM phase status mainly to solid for most of the period. Figure 8a,b, show the comparison between experimental and simulated temperature trends inside the PCM box for the warm season and cold season campaigns, respectively. A very good agreement between experimental and simulated data was observed for both periods, confirming the correct simulation of the boxes and the PCM.

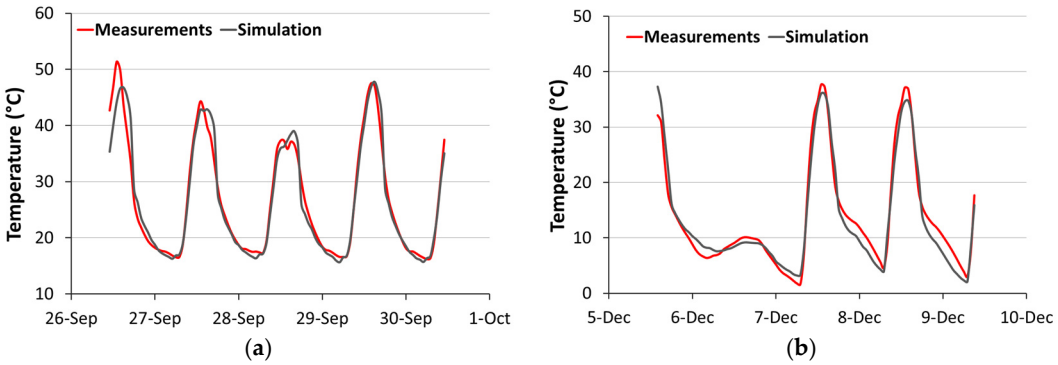

Figure 8. Measured and simulated air temperature, inside the PCM box for the warm season (**a**) and cold season (**b**) monitoring campaign.

In Figure 8b, a major difference between experimental and simulated temperature was observed during the night, when the air temperature inside the PCM box fell below 18 °C. In this period, the PCM material was in the solid phase and it continued to cool down. The model did not seem to follow the experimental trend in the same way as during the warm season campaign. This is probably because the PCM specifications were not available in the model for such low temperatures.

During the overcast day, temperatures were too low so that the PCM always stayed in the solid phase (Figure 8b). Root mean square error (RMSE) and normalized RMSE (NMRSE) are the indexes used to evaluate the accuracy of simulation.

Their definition is the following:

$$\mathrm{RMSE} = \sqrt{\frac{\sum_{\mathrm{i}=1}^{\mathrm{n}} \left(x_i^m - x_i^s\right)^2}{\mathrm{n}}} \tag{1}$$

$$\mathrm{NRMSE} = \frac{\mathrm{RMSE}}{x_{max}^m - x_{min}^m} \tag{2}$$

where m and s mean "measured " and "simulated", respectively, and max and min represent the maximum and minimum values of the variable in the time interval considered.

Table 6 lists the results. Three full days for each campaign were used to calculate the indexes discarding the first and last hours of operation. In addition, the indexes referring to the REF box were evaluated to verify the correct simulation of the box itself. NRMSE stays below 6% for all cases confirming the optimum agreement.

Table 6. RMSE and NMRSE between measured and simulated temperature trends for the two campaigns.

x	Ref Box		PCM Box	
Campaign	**RMSE (°C)**	**NMRSE (%)**	**RMSE (°C)**	**NMRSE (%)**
26-29/09/16	1.78	4.1	1.57	5.0
05-12/12/16	2.50	5.2	1.83	5.1

3.3. PCM Energy Saving Potential Assessment

Three different PCM panels were positioned on the floor of each office room of the STD building, as sketched in Figure 1. Table 7 depicts the melting temperature ranges of the three panels. The other thermal properties are the same of SP21E as shown in Table 1. Only the heat storage capacity of SP24E and SP26E is 180 kJ/kg instead of 160 kJ/kg. Figure 9 shows the total delivered energy of the reference buildings (STD and NZEB) compared to that delivered for the STD building modified with the SP21E, SP24E and SP26E, for the three cities of interest (Trento, Rome and Palermo). Even if the use of PCM reduced the energy request, this reduction was not enough to reach NZEB conditions.

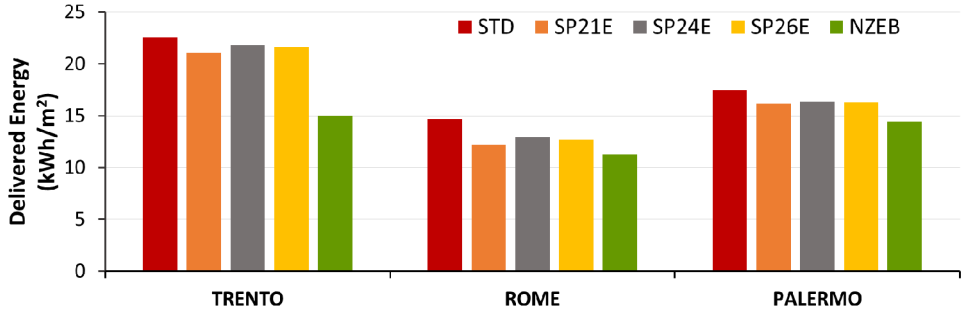

Figure 9. Delivered energy on an annual basis for the three PCM tested in the three cities compared to the STD and NZEB reference buildings.

Table 7. Melting and solidification temperature ranges for the three PCM tested.

Phase	SP21E	SP24E	SP26E
Melting (°C)	22−23	24−25	25−27
Solidification (°C)	21−19	23−21	25−24

This was particularly true for Trento, while for Rome, the goal was almost reached. Table 8 shows the percentage differences of energy saving (D) with respect to STD and NZEB buildings for the three PCM. In bold are the maximum savings obtained in Rome with SP21E (17%). In Trento and Palermo, SP21E outperformed STD with an improvement of 7% and 8%, respectively. A negative percentage means that the reference outperformed the other cases, as it was for NZEB for all PCM in the three cities. The lowest difference with respect to NZEB was in Rome with SP21E (−9%).

Table 8. Percentage difference of annual delivered energy of the buildings with the three PCM with respect to STD and NZEB reference buildings. Numbers in bold highlight the best percentage of energy saving.

City	SP21E		SP24E		SP26E		STD
	D_{STD} (%)	D_{NZEB} (%)	D_{STD} (%)	D_{NZEB} (%)	D_{STD} (%)	D_{NZEB} (%)	D_{NZEB} (%)
Trento	7	−40	3	−45	4	−44	−50
Rome	**17**	**−9**	12	−15	14	−13	−31
Palermo	8	−12	7	−13	7	−13	−22

It is interesting to look at the monthly values of delivered energy for the three locations to better understand the real behavior of PCM. From the energy analysis, it emerged that heating was the primary load for Trento, while in Rome and Palermo, cooling load was the most demanding. Table 9 shows the monthly delivered energy (heating and cooling) for Trento, Rome and Palermo. The STD performance was compared with the three PCM for each considered month. In the tables, green cells indicate the best performing PCM of the month, while bold numbers pertain to PCM subjected to

phase change during the month. It can be noted how SP21E was the best for all months in Trento, apart from February where STD slightly outperformed PCM. Moreover this material was in phase change for most of the time, owing to the low outside temperatures experienced at the location. During the coldest months, SP21E was mainly in the solid phase (no phase change observed). Also, SP24E experienced phase changes in June, July, September and October, while in August this was seen in SP26E. The maximum percentage difference in energy saving was observed during summer months where the energy consumption was the lowest.

Table 9. Delivered energy on a monthly basis for STD and the building provided with the three PCM for the city of Trento, Rome and Bolzano. Green cells highlight the best performing material for each month. Numbers in bold underline the months where the PCM is in phase change.

TRENTO												
	JAN	**FEB**	**MAR**	**APR**	**MAY**	**JUN**	**JUL**	**AUG**	**SEP**	**OCT**	**NOV**	**DEC**
	Delivered Energy (kWh/m^2)											
STD	3.72	3.49	3.46	2.23	0.95	0.35	0.18	0.39	0.55	1.17	2.69	3.38
SP21E	3.53	3.50	**3.40**	**2.19**	**0.92**	**0.18**	**0.02**	**0.09**	**0.30**	**0.98**	**2.59**	3.30
SP24E	3.62	3.52	3.44	2.24	0.97	**0.26**	**0.05**	0.12	**0.40**	**1.11**	2.68	3.36
SP26E	3.60	3.51	3.42	2.21	0.94	0.24	0.06	**0.16**	0.39	1.09	2.67	3.34
ROME												
	JAN	**FEB**	**MAR**	**APR**	**MAY**	**JUN**	**JUL**	**AUG**	**SEP**	**OCT**	**NOV**	**DEC**
	Delivered Energy (kWh/m^2)											
STD	1.09	0.76	0.43	0.23	0.55	1.56	2.87	3.12	1.86	0.98	0.49	0.75
SP21E	**0.97**	**0.59**	**0.28**	**0.10**	0.26	1.34	2.71	2.94	1.59	0.69	**0.16**	**0.57**
SP24E	1.06	0.69	0.35	**0.13**	**0.16**	1.40	2.81	3.05	1.75	**0.69**	**0.20**	0.68
SP26E	1.02	0.66	0.33	0.12	**0.25**	**1.15**	**2.72**	3.00	**1.74**	**0.74**	0.27	0.67
PALERMO												
	JAN	**FEB**	**MAR**	**APR**	**MAY**	**JUN**	**JUL**	**AUG**	**SEP**	**OCT**	**NOV**	**DEC**
	Delivered Energy (kWh/m^2)											
STD	0.35	0.22	0.13	0.25	0.69	2.14	3.45	4.64	2.86	1.95	0.57	0.27
SP21E	**0.25**	**0.10**	**0.05**	0.09	0.49	2.00	3.51	4.62	2.73	1.77	0.44	**0.10**
SP24E	**0.31**	**0.15**	**0.06**	**0.03**	**0.42**	2.10	3.42	4.63	2.82	1.77	**0.48**	**0.12**
SP26E	0.30	0.15	0.05	**0.06**	**0.40**	**1.87**	3.50	4.62	2.79	1.89	**0.47**	0.18

In Rome, SP21E was always the best performing PCM apart from May and June, where SP24E and SP26E performed the best, respectively. During winter months SP21E was in phase change, while SP24E and SP26E were in phase change in May and June. From July to October the same materials were in the temperature range near the phase change, but surprisingly they were not the best performing with respect to energy saving. The best performance of PCM in terms of energy saving was observed for the months of the intermediate seasons. SP24E and SP26E performed the best during summer months in Palermo, due to the higher outside temperatures. However, the improvement in energy saving during summer months was not significant, while it was more effective for intermediate seasons and winter months.

The temperature of PCM was compared to the temperature of the surface floor without PCM (STD building) to better understand the different performances among the various PCM and to explain the PCM gains. As an example, we showed the temperature trends for the month of June in Rome, where SP26E gave the best performance, as shown in Table 9.

Figure 10 shows the temperature trends experienced inside an office room positioned in the central part of the office building and provided with SP21E (a), SP24E (b) and SP26E (c). Melting and solidification temperature ranges are evidenced with yellow and light blue lines, respectively. Temperature of the various PCM (black line) is compared with temperature of the floor of STD building,

without PCM, (red line), also outside air temperature is presented (T_{air}). It can be noted that the capacity of PCM of storing energy in sensible or latent heat can be identified by observing its temperature trend. Indeed when heat is stored, the trend showed maximum and minimum temperature peaks with a similar behavior to the floor temperature of STD (Figure 10a,b).

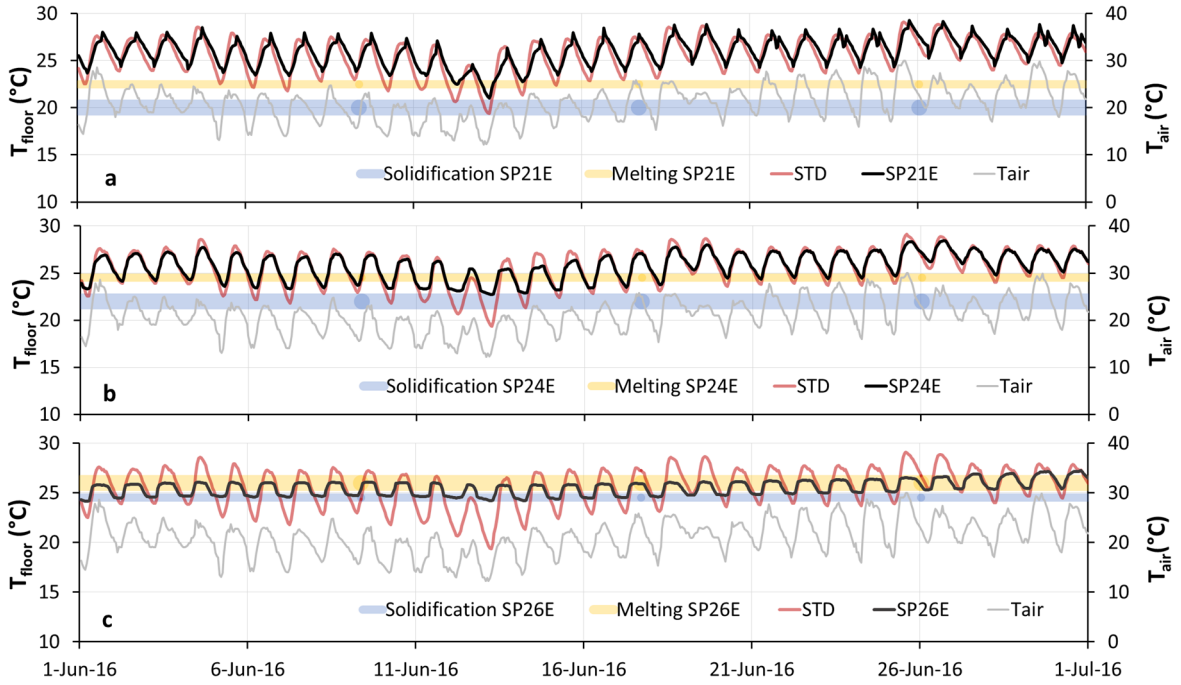

Figure 10. Floor temperatures compared to melting and solidification temperature range of PCM for the month of June in Rome: (**a**) SP21E; (**b**) SP24E; (**c**) SP26E.

On the contrary, when latent heat is stored, these peaks disappeared, since the temperature was fixed to the phase change temperature. This was observed for SP26E (Figure 10c), since the material was working perfectly in its phase change range for most of the time, guaranteeing the best performance with respect to STD. The temperature of SP21E, instead, always ranged outside its phase change temperature interval, indicating that the material was mainly working in mono phase state (liquid). In this case, PCM acted like a thermal mass and the heat storage was mainly due to heat. The same thing occurred for SP24E, even if for a certain amount of time it reached the melting phase.

From the observation of the PCM temperature trends as the ones in Figure 10, for all months and all cities, some conclusions could be drawn. The performance of PCM not only depends on the phase transition of the material but it also seemed to depend on the extent of the temperature range experienced by the material during the day/night cycle, and also on the absolute values of the maximum and minimum daily temperature peaks. These variables influenced the results differently between winter and summer. For this reason, PCM was effective both as latent and sensible heat storage systems. In the case of Figure 10 (summer period, June in Rome) the small temperature range variation of SP26E due to its phase change was beneficial to energy consumption, since this floor temperature induced a reduction in cooling demand. In August in Rome, instead, all PCM were far from phase change due to high temperatures (Figure 11). In these conditions the best performing material was SP21E because it has less thermal capacity than the other PCMs and can reach lower temperatures in the liquid phase during the night, reducing the heating effect that is typical of high capacity materials in summer. In winter, considering Rome as an example, the daily temperature range was suitable for phase change in SP21E so that its temperature was locked around 21 °C for most of the time, maintaining a floor configuration that helped to save heating.

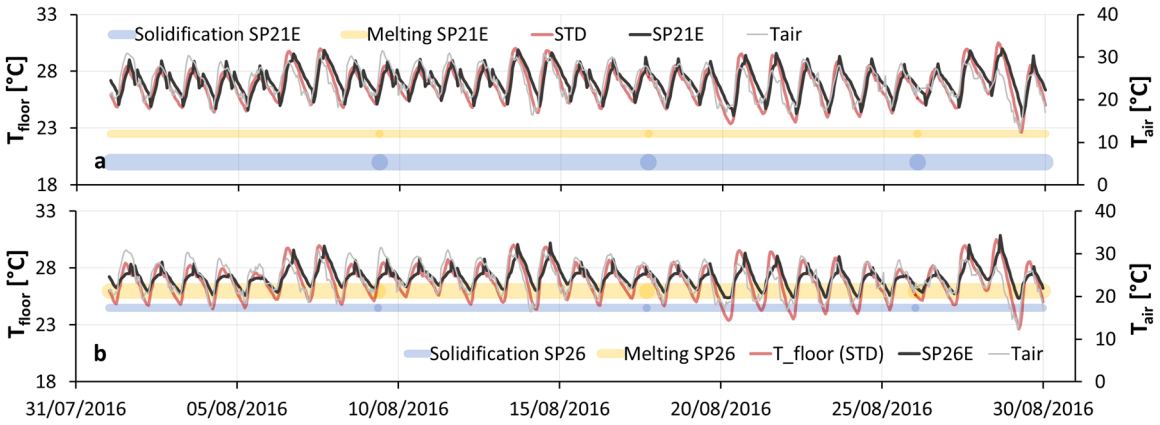

Figure 11. Floor temperatures compared to melting and solidification temperature range of PCM for the month of August in Rome: (**a**) SP21E; (**b**) SP24E.

Nevertheless, in November (Figure 12) thermal conditions were suitable for the SP24E phase change so the material temperature was locked around 24 °C. However SP21E, for some days of the months, was in the liquid phase and reached higher temperatures than SP24E during the day, acting as a more effective heat source than SP24E.

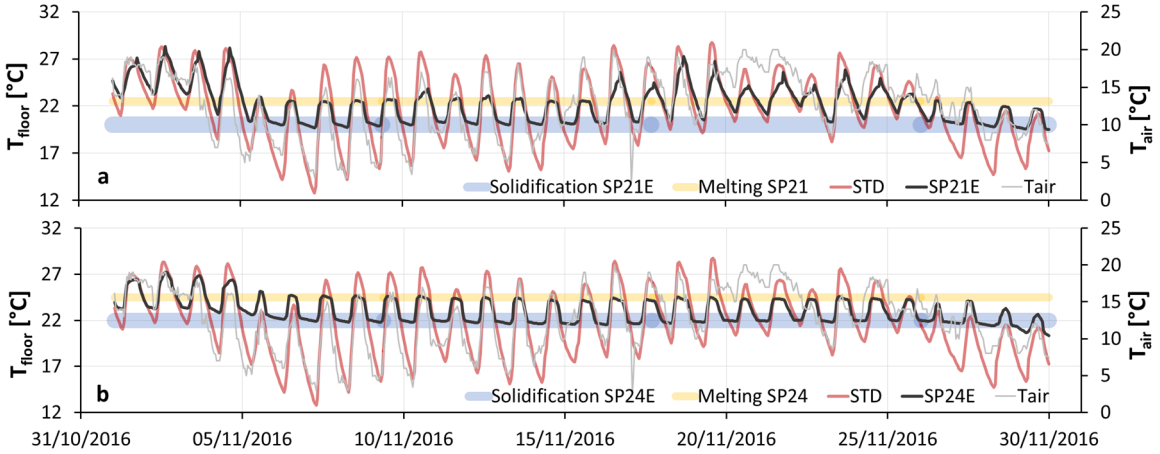

Figure 12. Floor temperatures compared to melting and solidification temperature range of PCM for the month of November in Rome: (**a**) SP21E; (**b**) SP24E.

Moreover, during the night, SP21E minimum temperature was similar to SP24E. This explained why SP21E prevailed as an energy saving material on an annual basis.

The PCMs worked both in winter and summer, as mentioned while discussing the monthly energy performance behavior. The STD building heat balance of one office room was compared to the case of a building implemented with SP21E, to better explain how PCM works during the winter in Trento, as an example (Figure 13). In this case, the material works as sensible heat storage.

It can be seen from Figure 13 that the power request for heating (HVAC) in the STD building was mainly during the night, since the inside air temperature fell below 12 °C (lower set point for heating outside office hours).

When SP21E was placed into the building [HVAC (SP21E)], the heating power requirement was reduced with respect to STD, since PCM released the heat absorbed during the day, increasing the inside air temperature during night.

For example, on the 12th of January, the release of approximately 200 W by PCM produces almost an annulment of the heating power.

On the contrary, a certain amount of heating is needed for PCM at the end of the day, because the material was absorbing heat from both solar radiation, and the HVAC system so that more power is requested to guarantee the set point temperature in the room. Indeed, as soon as solar radiation is not available, and in the likely case of low solar gains if compared to other thermal losses, the higher heat capacity of the room would require an additional heat source (as clearly visible in Figure 13). Nevertheless, the balance between heating reduction (at night and early morning) and heating request (at the end of the day) summarizes to a PCM monthly power request that is lower than STD.

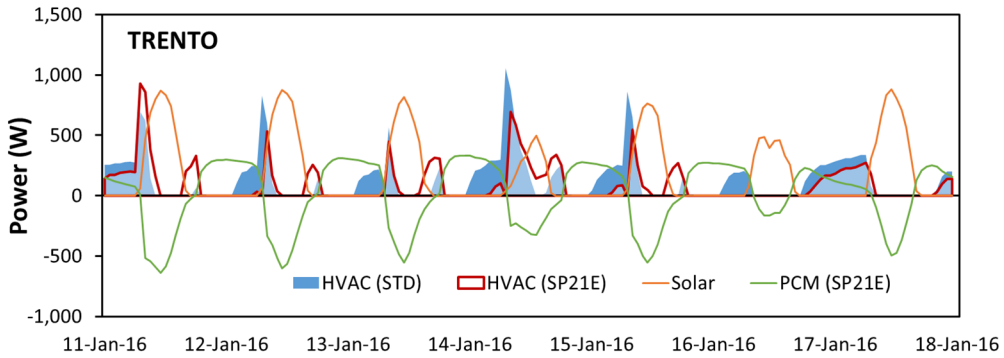

Figure 13. PCM acting in heating mode. Example of heat balance for a week in January in the city of Trento.

Figure 14a reports, as an example, the heat balance for a week of June in Rome to explain the PCM behavior for the cooling period.

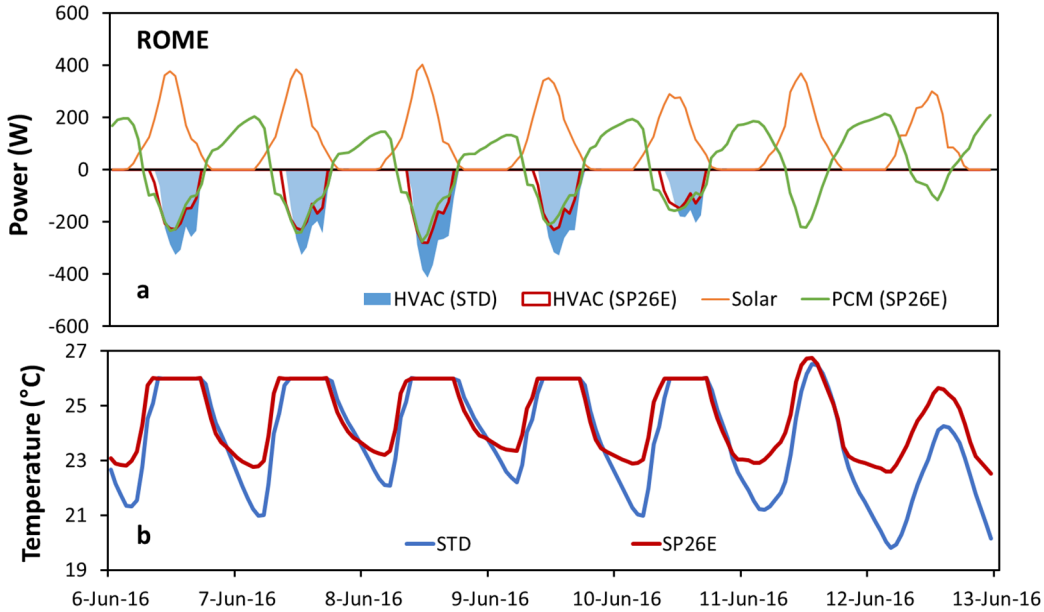

Figure 14. PCM acting in cooling mode. Example of a week of June in Rome: (**a**) heat balance; (**b**) inside air temperature for STD and SP26E.

In this case, SP26E produced the best performance (Table 9) and was always in phase transition. In the figure, the air temperature reached inside the STD office room and STD office room with SP26E are also plotted (Figure 14b).

The reduction of cooling power due to PCM was clearly visible during the days of the week, while during the weekend, no cooling was requested for both STD and SP26E, since the set point temperature was set to 28 °C, and outside temperature decreased in those days.

The increase in temperature of SP26E during the night (almost 3 °C) was due to heat release during solidification, while during the day, SP26E absorbed heat, reducing the cooling power needed (both temperatures stayed at set point).

During the weekend, as showed in Figure 14b, inside air temperature reached by SP26E was higher than STD. This is because PCM kept its phase change temperature, acting like a heat source inside the room.

In the present analysis, air infiltration of 0.6 ACH was taken into consideration. Night ventilation during the cooling period could improve the performance of PCM that in several cases was not able to discard completely the heat stored during the day. Indeed this solution proved to be effective for energy saving improvements [21].

In the cited case, however, night ventilation was applied only to the building provided with PCM and not to the reference. But it should be considered that night ventilation could be a valid means to reduce heat during the warm season even if the PCM material was not applied. To verify these assumptions, night ventilation was applied for the city of Rome. Windows were opened during the night from midnight till 7 a.m. for all cases (STD, NZEB, SP21E, SP24E and SP26E) and the calculations were made for the months from June till September. Figure 15 shows the delivered energy for cooling with night ventilation (NV) and without night ventilation (NO NV).

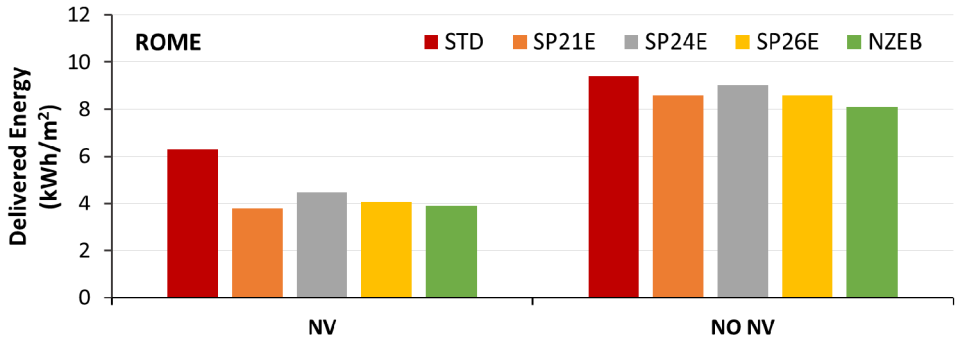

Figure 15. Delivered energy for cooling period for the three PCM tested in Rome compared to the STD and NZEB reference buildings, considering and not considering night ventilation.

A considerable reduction of delivered energy was observed for the NV case for all configurations. SP21E was confirmed to be the best performing material and in this case it also outperformed the NZEB reference building. Indeed, SP21 reduced cooling demand by 39% with respect to STD, and by 2% with respect to NZEB.

4. Conclusions

The work presented had the double objective of providing valuable experimental data to characterize the behavior of PCMs in real operating conditions, and to assess the energy saving potential of PCM panels laid on the floor of an office building as a retrofit solution. This analysis was carried out using a custom PCM software tool in the IDA ICE environment validated with the experimental data provided by the characterization analysis. Few works in the literature use validated tools to analyze the behavior of PCM for energy efficiency in buildings. The method proposed for the validation provided reliable results with a NRMSE below 5% between measured and simulated data. The capability of energy saving of PCM with three different melting points (SP21E, SP24E and SP26E) was investigated on a reference office building (STD) with characteristics that complied with the Italian norm (2005). The results were compared to the reference building prescribed by the more

recent 2015 Italian norm that states the minimum requirements of the building envelope to be NZEB. The results showed that none of the three PCM, if used as retrofit solution into the STD building, could reach the NZEB minimum requirements in terms of delivered energy for the cities of Trento, Rome, and Palermo in Italy. However, the retrofit with PCM, compared to STD, introduced a significant annual energy saving in Rome (17%), while for Trento and Palermo, a value of 7% and 8% respectively was reached. SP21E was the best performing PCM for all cities. The behavior of PCM in heating and cooling mode was investigated and explained. The performance of PCM does not depend only on the material phase transition but also on the extent of the temperature range experienced by the material during the day/night cycle, and at absolute values of the maximum and minimum daily temperature peaks. These variables influenced the results in a different way in winter and summer. For this reason, the tested PCM can be effective both as latent and sensible heat storage systems. In Trento, apart from the coldest months in winter, SP21E worked in the phase transition range, producing the best performance. During the coldest months all PCM, are in solid phase, however SP21E showed smaller temperature ranges, giving the best energy performance. In Rome and Palermo, during the cold season, SP21E was in phase change, giving the best results. For April and March in Rome, SP21E was still in phase transition, obtaining the best performance. In May and June, SP24E and SP26E exhibited phase changes, with the best results in terms of energy saving. In July and August, all PCM were in the liquid phase; however SP21E showed minimum temperatures in the night, slightly lower than the other PCM, producing the best results.

In Palermo for the same months (intermediate and summer) almost the same behavior was observed as for Rome; however the high temperatures in the warm season kept PCM in the liquid phase for a longer period than Rome, from July to October. It was also demonstrated that night ventilation is an essential means to reach NZEB minimum requirements, as evidenced by the case of Rome during the summer months.

Acknowledgments: Authors wish to thank RUBITHERM® for providing PCM panels for experimental tests as well as PCM specifications for dynamic simulation. A special thank also to the academic editors for their fruitful comments and suggestions giving a high contribution to improve the quality of the paper.

Author Contributions: Cristina Cornaro conceived and designed the experiments; Daniele Roncarati performed the experiments; Cristina Cornaro, Marco Pierro analyzed the data; Valerio Adoo Puggioni contributed software tools; Cristina Cornaro wrote the paper.

Conflicts of Interest: The authors declare no conflict of interest.

References

1. Telkes, M. Thermal storage for solar heating and cooling. In Proceedings of the Workshop on Solar Energy Storage Subsystems for the Heating and Cooling of Buildings, Charlottesville, VA, USA, 16–18 April 1975.
2. Khadiran, T.; Hussein, M.Z.; Zainal, Z.; Rusli, R. Advanced energy storage materials for building applications and their thermal performance characterization: A review. *Renew. Sustain. Energy Rev.* **2016**, *57*, 916–928. [CrossRef]
3. Souayfane, F.; Fardoun, F.; Biwole, P.H. Phase change materials (PCM) for cooling applications in buildings: A review. *Energy Build.* **2016**, *129*, 396–431. [CrossRef]
4. Kenisarin, M.; Mahkamov, K. Passive thermal control in residential buildings using phase change materials. Renew. *Sustain. Energy Rev.* **2016**, *55*, 371–398. [CrossRef]
5. Lee, S.H.; Yoon, S.J.; Kim, Y.G.; Choi, Y.C.; Kim, J.H.; Lee, J.G. Development of building materials by using micro-encapsulated phase change material. *Korean J. Chem. Eng.* **2007**, *24*, 332–335. [CrossRef]
6. Zhang, G.H.; Bon, S.A.; Zhao, C.Y. Synthesis, characterization and thermal properties of novel nanoencapsulated phase change materials for thermal energy storage. *Sol. Energy* **2012**, *86*, 1149–1154. [CrossRef]
7. Zhang, Z.; Shi, G.; Wang, S.; Fang, X.; Liu, X. Thermal energy storage cement mortar containing n-octadecane/expanded graphite composite phase change material. *Renew. Energy* **2013**, *50*, 670–675. [CrossRef]

8. Li, M.; Wu, Z.; Tan, J. Heat storage properties of the cement mortar incorporated with composite phase change material. *Appl. Energy* **2013**, *103*, 393–399. [CrossRef]
9. Marchi, S.; Pagliolico, S.; Sassi, G. Characterization of panels containing micro-encapsulated Phase Change Materials. *Energy Convers. Manag.* **2013**, *74*, 261–268. [CrossRef]
10. Barreneche, C.; Navarro, M.E.; Fernández, A.I.; Cabeza, L.F. Improvement of the thermal inertia of building materials incorporating PCM. Evaluation in the macroscale. *Appl. Energy* **2013**, *109*, 428–432. [CrossRef]
11. Tardieu, A.; Behzadi, S.; Chen, J.J.J.; Farid, M.M. Computer simulation and experimental measurements for an experimental PCM-impregnated office building. In Proceedings of the Building Simulation 2011: 12th Conference of International Building Performance Simulation Association, Sydney, Australia, 14–16 November 2011.
12. Entrop, A.G.; Brouwers, H.J.H.; Reinders, A.H.M.E. Experimental research on the use of micro-encapsulated Phase Change Materials to store solar energy in concrete floors and to save energy in Dutch houses. *Sol. Energy* **2011**, *85*, 1007–1020. [CrossRef]
13. Su, J.F.; Wang, X.Y.; Wang, S.B.; Zhao, Y.H.; Huang, Z. Fabrication and properties of microencapsulated-paraffin/gypsum-matrix building materials for thermal energy storage. *Energy Convers. Manag.* **2012**, *55*, 101–107. [CrossRef]
14. Sage-Lauck, J.S.; Sailor, D.J. Evaluation of phase change materials for improving thermal comfort in a super-insulated residential building. *Energy Build.* **2014**, *79*, 32–40. [CrossRef]
15. Goia, F.; Perino, M.; Serra, V. Experimental analysis of the energy performance of a full-scale PCM glazing prototype. *Sol. Energy* **2014**, *100*, 217–233. [CrossRef]
16. Fernandes, N.T.A.; Costa, V.A.F. Use of Phase-Change Materials as Passive Elements for Climatization Purposes in Summer: The Portuguese Case. *Int. J. Green Energy* **2009**, *6*, 302–311. [CrossRef]
17. Zwanzig, S.D.; Lian, Y.; Brehob, E.G. Numerical simulation of phase change material composite wallboard in a multi-layered building envelope. *Energy Convers. Manag.* **2013**, *69*, 27–40. [CrossRef]
18. Zhou, D.; Shire, G.S.F.; Tian, Y. Parametric analysis of influencing factors in Phase Change Material Wallboard (PCMW). *Appl. Energy* **2014**, *119*, 33–42. [CrossRef]
19. Guarino, F.; Athienitis, A.; Cellura, M.; Bastien, D. PCM thermal storage design in buildings: Experimental studies and applications to solaria in cold climates. *Appl. Energy* **2017**, *185*, 95–106. [CrossRef]
20. Ascione, F.; Bianco, N.; De Masi, R.F.; de' Rossi, F.; Vanoli, G.P. Energy refurbishment of existing buildings through the use of phase change materials: Energy savings and indoor comfort in the cooling season. *Appl. Energy* **2014**, *113*, 990–1007. [CrossRef]
21. Seong, Y.B.; Lim, J.H. Energy saving potentials of phase change materials applied to lightweight building envelopes. *Energies* **2013**, *6*, 5219–5230. [CrossRef]
22. Guarino, F.; Dermardiros, V.; Chen, Y.; Rao, J.; Athienitis, A.; Cellura, M.; Mistretta, M. PCM thermal energy storage in buildings: Experimental study and applications. *Energy Procedia* **2015**, *70*, 219–228. [CrossRef]
23. Björsell, N.; Bring, A.; Eriksson, L.; Grozman, P.; Lindgren, M.; Sahlin, P.; Sha-povalov, A.; Vuolle, M. IDA indoor climate and energy. In Proceedings of the Building Simulation Conference, Kyoto, Japan, 13–15 September 1999.
24. Italian norm. In *Interministerial Decree 26 June 2015—Application of Calculation Methodologies for Energy Performance and Definition of Prescription for Minimum Requirements of Buildings*; Italian Government: Rome, Italy, 2015.
25. Italian Legislative Decree n. 192/05. In *Attuazione Della Direttiva 2002/91/CE Relativa al Rendimento Energetico Nell'edilizia*; Italian Government: Rome, Italy, 2005; pp. 1–28.
26. Cornaro, C.; Bucci, F.; Pierro, M.; Bonadonna, M.E.; Siniscalco, G. A new method for the thermal characterization of transparent and semi-transparent materials using outdoor measurements and dynamic simulation. *Energy Build.* **2015**, *104*, 57–64. [CrossRef]
27. Spena, A.; Cornaro, C.; Serafini, S. Outdoor ESTER test facility for advanced technologies PV modules. In Proceedings of the 2008 33rd IEEE Photovoltaic Specialists Conference, San Diego, CA, USA, 11–16 May 2008.
28. Cornaro, C.; Pierro, M.; Roncarati, D.; Puggioni, V.A. Validation of a PCM simulation tool in IDA ICE dynamic building simulation software using experimental data from Solar Test Boxes. Pre-prints of BSA 2017—Building Simulation Applications. In Proceedings of the Building simulation Applications (BSA), Bolzano, Italy, 8–10 February 2017.

29. Rubel, F.; Kottek, M. Comments on: The thermal zones of the Earth by Wladimir Köppen (1884). *Meteorol. Z.* **2011**, *20*, 361–365. [CrossRef]
30. Nielsen, T.R.; Rosenfeld, J.L.J.; Svendsen, S. *A Simple Energy Rating for Solar Shading Devices*; Technical University of Denmark: Copenhagen, Denmark, 2003.
31. Cornaro, C.; Basciano, G.; Puggioni, V.; Pierro, M. Energy Saving Assessment of Semi-Transparent Photovoltaic Modules Integrated into NZEB. *Buildings* **2017**, *7*, 9. [CrossRef]
32. European Committee of Standardization. Part 1: Indoor Work Places. In *Standardization EN12464-1:2011 Light and Lighting—Lighting of Workplaces*; European Committee of Standardization: Brussels, Belgium, 2011.